Uniform GTD와 Aperture Integration을 이용한 내부에 Terminator가 있는 평면도파관의 전자기파의 산란

○명 노 훈

한국과학기술대학

A Uniform GTD and Aperture Integration Analysis of the Electromagnetic Scattering by a Semi-infinite Parallel Plate Waveguide with an Interior Termination and Lossy Inner Walls

N. H. Myung

Korea Institute of Technology

< Abstract >

A solution which combines ray and aperture integration(AI) techniques is presented for the problem of electromagnetic plane wave scattering by an open-ended, perfectly-conducting, semi-infinite parallel plate waveguide with a thin, uniform layer of lossy or absorbing material on its inner walls, and with a simple planar termination inside. Numerical results are given for the fields outside the waveguide.

I. Introduction

The fields scattered back into the exterior region by the edges of the semi- infinite parallel plate waveguide of Figure 1 as well as the fields coupled into the interior region are described here in terms of the rays diffracted by the edges and by the rays which propagate inside the waveguide, respectively. The field from a source point to an observation point is tracked along ray paths in the ray method; these rays obey the rules of geometrical optics.

The fields radiated out from the open-end of the waveguide after reflecfting from the interior termination are calculated by a combination of the ray method and an aperture integration(AI) technique together with the use of an equivalence theorem. An $e^{+j\omega t}$ time dependence is assumed and suppressed in this analytical development.

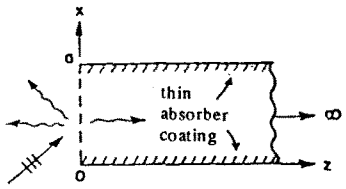

Figure 1. Scattering of an electromagnetic plane wave by an open-ended semi-infinite parallel plate waveguide.

II. Interior fields

A simple planar termination which is L wavelengths away from the open-end is placed inside the waveguide as shown in the Figure 2. The field at the observation point consists of two groups of rays. One group is associated with the incident, reflected and diffracted rays from the open-end of the waveguide as in the case of the waveguide without a termination. The other group of rays corresponds to those which are reflected back from the termination and then reach the field point. The ray field due to the reflection by the termination can be calculated by simply using an effective observation point at an image location which is symmetrical with respect to the actual observation point P about the termination as shown in Figure 2. Thus the ray field at P is calculated

by adding each ray from the open-end reaching P and P′ by applying the reflection coefficient of the termination wall to those rays reaching P′.

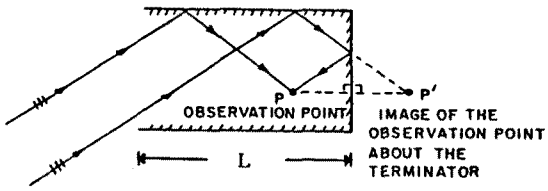

Figure 2. A parallel plate waveguide with a planar termination.

III. Exterior fields

The field outside the semi-infinite parallel plate waveguide with a planar termination inside is calculated using an AI technique together with the use of equivalence theorem [1, 2, 3] in this section. In order to use AI to calculate the field, the surface equivalent currents J_s and/or M_s are determined over the aperture (open-end) of the waveguide. These equivalent currents can be obtained as follows.

Let a line dipole dp_e radiate the fields E and H in the presence of the open-ended parallel plate waveguide as shown in Figure 3. One can use the

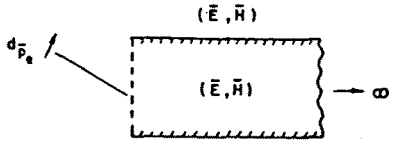

Figure 3. Radiation of a dipole dp_e in the presence of the open-ended parallel plate waveguide.

equivalent currents J_s and M_s on the aperture and walls of the waveguide according to the equivalence theorem. These surface equivalent currents radiate the field E and H outside the waveguide and null field inside region as shown Figure 4. Over the surface, the equivalent currents are given by

$$J_s = \hat{n} \times H_a \qquad (1)$$
$$M_s = E_a \times \hat{n}$$

where H_a (or E_a) is the tangential magnetic (or electric) field over the aperture (open-end) of the waveguide and $\hat{n}$ is a unit normal vector pointing outward the waveguide.

Since the tangential componets of E do not exist on the waveguide wall, because of vanishing boundary conditions on the surface, only M_s over the aperture is non-zero as shown in the figure.

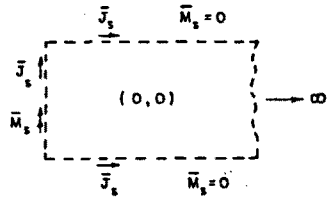

Figure 4. The equivalent model of Figure 3.

Furthermore, since the radiated field by J_s on the waveguide wall is expected to be very weak in the broadside (-z direction), J_s is neglected for the radiated field outside the waveguide. Consequently, J_s and M_s, over the aperture in Figure 4 would radiate outward. Next, consider that the imaginary infinite plane of an electric conductor approaches the aperture. Then it shorts out the equivalent current J_s, and only M_s radiates in the presence of the conductor. By image theory, the conductor can be removed and replaced by the image source M_s as shown in Figure 5(a). Since the

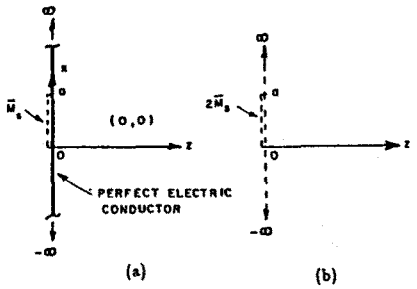

Figure 5. Equivalent model for magnetic source radiation near a perfect electric conductor.

imaginary source is in the same direction as the equivalent source, the equivalent problem of Figure 5(a) reduces to that of Figure 5(b). Then the magnetic current M_s radiates in a unbounded medium and it is represented by

$$2\,M_s = 2\,E_a \times \hat{n} \tag{2}$$

Next, an appropriate radiation integral is employed to calculate the fields outside the waveguide. The analysis of this radiation problem is described in detail as below.

Consider a ray tube which after being reflected from the termination occupies the portion $a_1<x<a_2$ in the aperture in Figure 6. Also, the angle at which this ray tube arrives in the aperture is $\pi+\phi'$ as shown in the figure. The electric field at the aperture is then given by

$$E_a = \begin{cases} \hat{y}\, E_{ao}\, e^{-jk[(n+1)\,a\sin\phi'+2L\cos\phi']} \cdot e^{jkx\sin\phi'} \\ \qquad\qquad ;\text{for odd } n \\ \hat{y}\, E_{ao}\, e^{-jk[na\sin\phi'+2L\cos\phi']} \cdot e^{-jkx\sin\phi'} \\ \qquad\qquad ;\text{for even } n \end{cases} \tag{3}$$

where

E_{ao} : electric field strength of the reflected ray tube in the aperture; this is a known quantity.

L : distance from the open-end to the termination

a : waveguide height

n : number of reflections of a ray tube

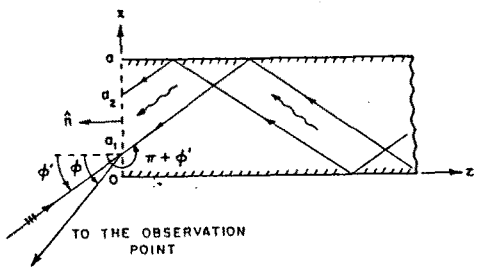

Figure 6. A ray tube reflected back from the termination.

If a perfect electric conductor is placed behind the aperture such that $J_s=0$ as mentioned earilier, the M_s for odd values of n is given by

$$2\,M_s = -2\,\hat{x}\,E_a\, e^{-jk[(n+1)\,a\sin\phi'+2L\cos\phi']} \cdot e^{jkx\sin\phi'} \tag{4}$$

An appropriate 2-D radiation integral is given by

$$E^s = \sqrt{\frac{jk}{8\pi}}\, Z_o \int Y_o\, \hat{R} \times 2\,M_s\, \frac{e^{-jkR}}{\sqrt{R}}\, dl' \tag{5}$$

where Z_0 (or Y_0) is free-space wave impedance (or admittance) and R is a unit vector in radiation direction. Since $J_s=0$ in the case considered here, E_y^s radiated in the far zone exterior to the aperture by the M_s in Equation (4) is represented as

$$E_y^s = \sqrt{\frac{jk}{8\pi}} \int_{a_1}^{a_2} \hat{y}\cdot(\hat{x}\times\hat{R})\, 2M_s\, \frac{e^{-jkR}}{\sqrt{R}}\, dx' \tag{6}$$

where

$$R = R_0 - x'\sin\phi$$

$$\hat{R} = -\hat{x}\sin\phi - \hat{z}\cos\phi$$

in the far zone case. Also, ϕ is an observation angle and R_0 is the distance from the origin to the observation point. Hence, Equation (6) reduces to

$$E_y^s = \sqrt{\frac{jk}{2\pi}}\, E_{ao}\, e^{-jk[(n+1)\,a\sin\phi'+2L\cos\phi']}\cos\phi\,\frac{e^{-jkR_0}}{\sqrt{R_0}} \int_{a_1}^{a_2} e^{jkx'(\sin\phi+\sin\phi')}\, dx'$$

$$= \sqrt{\frac{jk}{2\pi}}\, E_{ao}\, e^{-jk[(n+1)\,a\sin\phi'+2L\cos\phi']}\cos\phi\,\frac{e^{-jkR_0}}{\sqrt{R_0}} \cdot 2d_1\,\frac{\sin x_1^o}{x_1^o}\, e^{jkx_2^o} \tag{7}$$

where

$$x_1^o = kd_1(\sin\phi+\sin\phi')$$

$$x_2^o = kd_2(\sin\phi+\sin\phi')$$

$$d_1 = \frac{a_2-a_1}{2}$$

$$d_2 = \frac{a_2+a_1}{2}$$

Similarly, the radiated field E_y^s for even values of n is expressed as

$$E_y^s = \sqrt{\frac{jk}{2\pi}}\, E_{ao}\, e^{-jk[na\sin\phi'+2L\cos\phi']}\cos\phi\,\frac{e^{-jkR_0}}{\sqrt{R_0}} \int_{a_1}^{a_2} e^{jkx'(\sin\phi-\sin\phi')}\, dx'$$

$$= \sqrt{\frac{jk}{2\pi}}\, E_{a0}\, e^{-jk|n\,a\sin\phi' + 2L\cos\phi'|}\, \cos\phi\, \frac{e^{-jkR_0}}{\sqrt{R_0}} \cdot 2d_1 \frac{\sin x_1^e}{x_1^e}\, e^{jkx_2^e} \qquad (8)$$

where

$$x_1^e = kd_1(\sin\phi - \sin\phi')$$

$$x_2^e = kd_2(\sin\phi - \sin\phi')$$

Note that the limits a_1 and a_2 in the integral of Equation (6) can be determined analytically and they are functions of an incident angle ϕ', a waveguide width a and the location of the termination at z=L. It is also noted that there are always two ray tubes to be considered over the aperture with different number of reflections and arrival angle (see Figure 7: one has n reflections with its arrival angle of $\pi+\phi'$ at the aperture and the other has n+1 reflections with arrival angle of $\pi-\phi'$. The total radiated field can then be obtained by superimposing each radiated field.

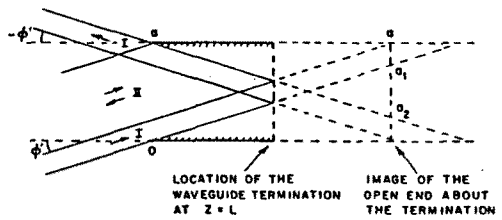

Figure 7. Rays incident on the open-end of the the waveguide.

IV. Numerical results.

As an illustration, radiation patterns for a far field are plotted as a function of radiation angle ϕ in Figures 8 and 9 for different values of ϵ and μ. Each radiation pattern has two peaks at $\phi=+30^\circ$ and $\phi=-30^\circ$ directions as expected. The level of the two peaks are slightly different from each other because the width of each ray tube on the aperture is different and one ray tube has one more reflection than the other inside the waveguide as mentioned earlier. Note that the radiation pattern for the case of Figure 8 is mainly due to the interior re-radiation. However, as the values of ϵ and μ becomes larger, the interior re-radiation becomes weaker and the diffracted fields due to the waveguide edges at the open-end contribute to the total scattered fields mainly.

In order to check the accuracy of the radiation patterns shown in Figures 8 and 9, the radiation patterns obtained by the ray solution developed in this section are compared with those obtained by the hybrid high frequency technique in conjunction with the multiple scattering method (MSM) [4, 5, 6] for the perfectly-conducting case. The analysis of MSM is based on a combination of asymptotic high frequency techniques such as ray method, the equivalent current method (ECM), and the physical theory of diffraction (PTD), with the usual modal techniques. As shown in the Figure 10, the two solutions show good agreement in the main and the first side lobe regions. The discrepancy in other regions is due to the fact that the diffracted rays in the interior re-radiation of the ray solution is not included for analytical simplicity in the present paper.

V. Conclusion

The ray method is simple in concept and analysis and it lends some physical insight into the propagation and scattering mechanisms particularly in connection with the coupling of the fiels from the exterior to the interior regions in the case of the semi-infinite waveguide configuration, as well as into the effect of the wall loss on the fields in the interior waveguide region. Also, the ray solution does not require one to evaluate the eigenvalues which are essential for the construction of the modal solution.

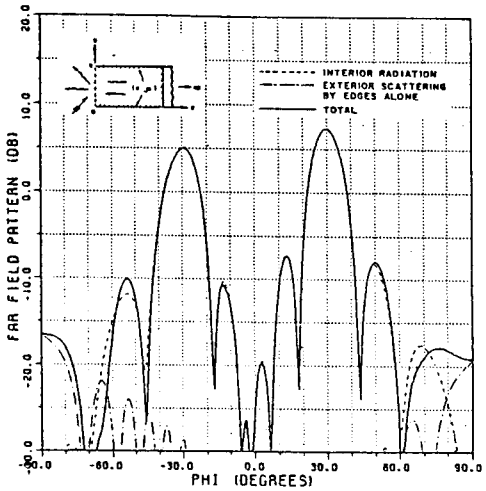

Figure 8. Radiation pattern for a far field of the parallel plate waveguide for TEy case.

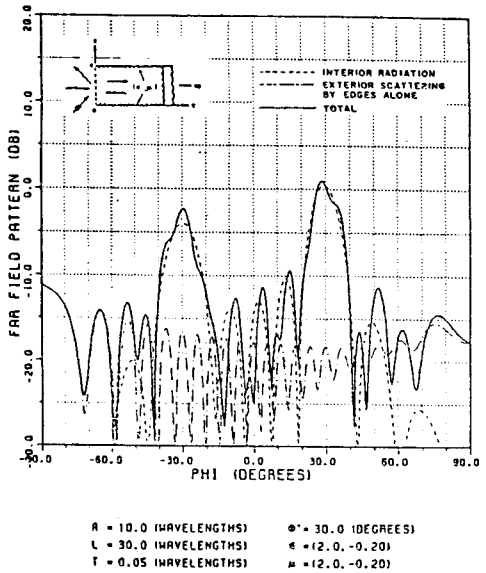

Figure 9. Radiation pattern for a far field of the parallel plate waveguide for TEy case.

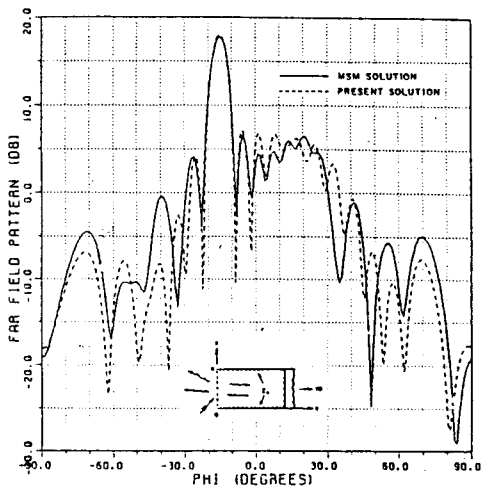

Figure 10. Comparison of the radiation patterns for a far field obtained by the ray and modal solutions.

< References >

1. R. F. Harrington, "Time Harmonic Electro-magnetic field", McGraw-Hill Book Co., New York, pp. 100-103, 143-263, 1961.

2. C. A. Balanis, "Antenna Theory, analysis and design", Harper and Row Publishers, New York, pp. 447-454, 1982.

3. E. V. Jull, "Aperture Antennas and Diffraction Theory", Peter Peregrinus Ltd., New York, 1981.

4. P. H. Pathak, A. Atintas, C. W. Chuang and S. Barkeshli, "Near Field Scattering by Rectangular and Circular Inlet Configurations with an Impedance Surface Termination", Final Report 715267-1, The Ohio State University, ElectroScience Laboratory, July 1984.

5. P. H. Pathak, C. W. Chuang, "Continuation of work on Near and Far Field Scattering by Rectangular and Circular Inlet Configurations with an Impedance Surface Termination", Final Report 715979-1, The Ohio State University, ElectroScience Laboratory, June 1985.

6. P. H. Pathak, C. W. Chuang, M. C. Liang, H. Wang, H. T. Kim, "Ram and Inlet Modeling Studies", Final Report 716495-2, The Ohio State University, ElectroScience Laboratory, October 1985.